21st IAEA Fusion Energy Conference
Chengdu, China, 16 - 21 October, 2006

IAEA-CN-149/ TH/P7-1

Analysis of Net Plasma Currents in Non-Axisymmetric Plasmas

Y. Nakamura et al.

NIFS-868 Oct. 2006

Analysis of Net Plasma Currents in Non-Axisymmetric Plasmas

Yuji Nakamura 1), K. Y. Watanabe 2), M. Yokoyama 2), N. Nakajima 2), A. Fukuyama 3), H. Funaba 2), Y. Suzuki 2), S. Murakami 3), K. Ida 2), S. Sakakibara 2), and H. Yamada 2)

1) Graduate School of Energy Science, Kyoto University, Uji, Japan
2) National Institute for Fusion Science, Toki, Japan
3) Graduate School of Engineering, Kyoto University, Kyoto, Japan

e-mail contact of main author: nakamura@energy.kyoto-u.ac.jp

Abstract. Net plasma currents and those time evolutions are studied numerically for non-axisymmetric plasmas. Based on the neoclassical transport theory, effects of the non-axisymmetry on the bootstrap (BS) current are investigated for a tokamak plasma which has toroidal field (TF) ripples. It is found that the BS current is reduced by a factor of a square root of the TF ripple ratio in a rippled tokamak. We also found that the reduction of the BS current due to TF ripples becomes small if we take the poloidal dependence of the TF ripple ratio into account. For helical plasmas, we have developed a net plasma current simulation code for integrated simulations, and analyze net plasma currents observed in a Large Helical Device (LHD) plasma. It is found that non-inductive currents can be sufficiently large to change the rotational transform profile at the plasma core region, even though the total current is too small to change the rotational transform at the plasma boundary. The effect of the inductive current is important for estimation of the net plasma current especially when the beam driven currents are considered.

1. Introduction

Efforts to develop an integrated simulation code for helical plasmas are underway [1], in order to analyze experimental data from the viewpoints of integrated physics and to draw up new experimental plans especially for burning plasma experiments. As a first step of the development, time evolution of the net plasma current, which is consistent with the three-dimensional (3D) magnetohydrodynamic (MHD) equilibrium, is considered by taking the non-inductive and inductive current into account.

Though the net plasma current is not necessary for MHD equilibrium in helical plasmas, finite net toroidal currents have been observed in actual experiments. It is considered that non-inductive currents such as bootstrap (BS) currents or beam driven currents are included in it. An asymptotic approach to the BS current in non-axisymmetric toroidal plasmas was described by Shaing and Callen [2], and its analytic expression in Boozer coordinates is given for the low collisionality regime by Shaing et al. [3]. Watanabe et al. [4,5] developed the SPBSC code using the asymptotic formula to study the BS current for LHD plasmas.

As a module of the integrated simulation code for helical plasmas, we have developed the BSC code [1] by improving the SPBSC code. This code uses a connection formula of asymptotic solutions for BS currents of non-axisymmetric plasmas in Pfirsch-Schülter, plateau, and low collisionality regimes. The BSC code has been applied to the analysis of the BS current observed in Heliotron J plasmas [6]. It was shown that the neoclassical transport theory can explain the experimental observation that the bumpy field component can change the direction of the BS current. In Ref. [7], we applied the BSC code to estimate the BS currents in a tokamak using a simple TF ripples model. In the present study, we show more detailed results on the effects of the TF ripples on the BS currents (Section 2).

In a neutral beam (NB) injected plasma, Ohkawa currents can also contribute to the net plasma current. Ohkawa currents are estimated by the BSC/FIT modules. Time evolution of non-inductive currents that is consistent to the 3D MHD equilibrium is calculated for an LHD plasma in Section 3. Here we consider BS currents and Ohkawa currents as the non-inductive currents. Effects of the inductive currents is discussed in Section 4.

2. Effects of the Toroidal Field Ripples on the Bootstrap Current in Tokamaks

It is pointed out that the toroidal field ripple, i.e. bumpy field component, reduces the bootstrap current in a tokamak [2]. This is because the symmetry breaking component reduces the BS currents and the neoclassical parallel flows which are driven by the parallel viscosity. As is shown in Refs. [2-5], the BS current's dependence on the magnetic configuration can be expressed in terms of the geometric factor $\tilde{G}_b$. The geometric factor can be calculated from the total poloidal current outside a flux surface G, the total toroidal current inside a flux surface I, the safety factor q, and the distribution of the magnetic field strength $B(\theta,\zeta)$ on a flux surface, and can be expressed in Boozer coordinates as [3,4]

$$\tilde{G}_b = \tilde{G}_b^{H_1} + \tilde{G}_b^{H_2} + \tilde{G}_b^{W},$$

where

$$\tilde{G}_b^{H_1} = \langle H_1 \rangle = (qG - I)/2,$$
$$\tilde{G}_b^{H_2} = H_2 (qG + I)/2,$$
$$\tilde{G}_b^{W} = -\frac{3}{4}\frac{q(qG+I)}{f_t}\int_0^1 \frac{\lambda W(\lambda)\mathrm{d}\lambda}{\left\langle\sqrt{1-\lambda B/B_{\max}}\right\rangle},$$
$$H_2 = \frac{\left\langle(\partial B/\partial\theta)^2\right\rangle - q^2\left\langle(\partial B/\partial\zeta)^2\right\rangle}{\left\langle(\partial B/\partial\theta + q\partial B/\partial\zeta)^2\right\rangle},$$

θ (ζ) is the poloidal (toroidal) angle in Boozer coordinates, and $\langle\cdot\rangle$ indicates the flux surface averaged quantity. The fraction of trapped particles f_t and $W(\lambda)$, whose explicit expressions are given in Ref. 4, are calculated from $B(\theta,\zeta)$. The term $\tilde{G}_b^{W}$ vanishes if the magnetic filed strength's distribution on a flux surface has any symmetry [8], such as axisymmetry or helical symmetry. Note that $\tilde{G}_b^{H_2}$ also contains asymmetric contribution through H_2, which is closely related to the direction of the grad-B drift, and it plays a dominant role in determininig the direction of the bootstrap current. If the configuration is axisymmetric, $B = B(\theta)$, H_2 becomes unity and $\tilde{G}_b^{tok} = qG$ can be obtained. This shows that all axisymmetric tokamaks have the same geometric factor whether they have a circular or D-shaped cross section, for example.

When we consider a rippled tokamak of which magnetic field strength is written by $B(\theta,\zeta) = B_0(1 - \varepsilon_t\cos\theta + \delta\cos(N\zeta))$, H_2 becomes $(\varepsilon_t^2 - N^2q^2\delta^2)/(\varepsilon_t^2 + N^2q^2\delta^2)$. If $\varepsilon_t \sim 0.3$, $q \sim 2$, $N \sim 18$, and $\delta \sim 0.01$, we can get $\varepsilon_t/(Nq\delta) \sim 0.83$ and $H_2 \sim -0.2$. In order to estimate the term $\tilde{G}_b^{W}$, numerical calculation is necessary. Since the TF ripples in tokamaks are usually small, we might neglect the third term containing $W(\lambda)$. However, this produces a significant reduction of the bootstrap current; $\tilde{G}_b/\tilde{G}_b^{tok} \sim 0.3$. This means that small symmetry-breaking components such as TF ripples might reduce the bootstrap currents to a notable degree. In Ref. [7], the numerical calculation has been done for the standard magnetic

field model of rippled tokamaks. An 8-15% reduction of the BS current is predicted in a tokamak plasma having $q = 1.8$ and $\varepsilon_t = 0.3$ when the TF ripple rate is 1-3%. Though such reduction is much smaller than the simple estimation, it still can not be ignored. The N dependence can be neglected for usual tokamak plasmas with $N \geq 15$. It should be noted that the N dependence can appeare through δ, in practice, because lower N gives larger δ in a realistic equilibrium.

Toroidicity ε_t and safety factor q dependence of the bootstrap current reduction due to TF ripples are shown in Fig.1 It is found that the q dependence is weak, but smaller ε_t enhances the BS current reduction. This means that the BS current reduction due to TF ripples might not be ignored even in the core region where the TF ripple rate is small, because toroidicity ε_t is also small there.

In actual tokamaks, the TF ripple rate has a poloidal dependence. To investigate the effect of poloidal dependence of TF ripple, the BS current calculation is done for the TF ripple model of $B(\theta,\zeta) = B_0(1 - \varepsilon_t \cos\theta + (\delta/2)(1+\cos\theta)\cos(N\zeta))$. In this model, TF ripple rate is δ at the outboard of torus ($\theta = 0$), but it becomes zero at the inboard of torus ($\theta = \pi$). The calculation shows that the reduction of the BS current due to TF ripple becomes smaller if we take the poloidal dependence of the TF ripple rate.

3. Non-inductive currents in helical plasmas

In order to estimate the time evolution of non-inductive current, the 3D MHD equilibrium calculation code VMEC and the non-inductive current calculation code BSC/FIT is solved alternately in time.

The BSC code has the following characteristics; (1) connection formula from $1/\nu$ to P-S collisional regime is applied, (2) bootstrap current is estimated based on momentum method for asymmetric devices proposed by K.C. Shaing et al. [3, 9], where the linearlized drift kinetic

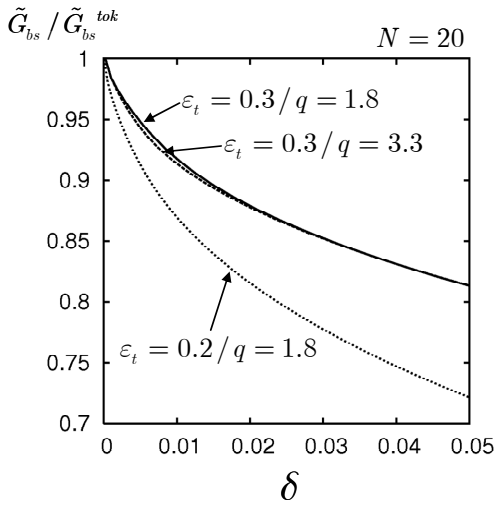

Fig.1 TF ripple dependence of the geometric factor of the bootstrap current.

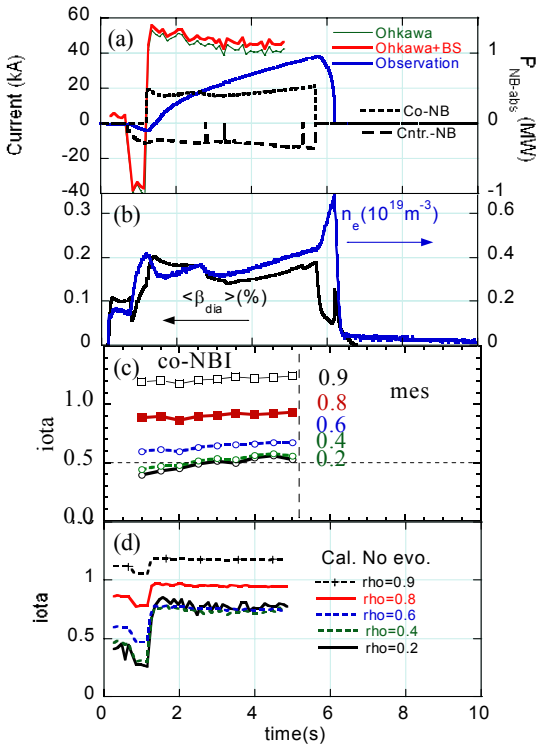

Fig.2 Waveform of the discharge with 2 NB-injection: (a) blue: observed current, red: calculated Ohkawa and bootstrap current, green: calculated Ohkawa current, dotted line and dashed line: absorbed beam power, (b) averaged beta and electron density, (c) rotational transform measured by MSE, (d) estimated rotational transform due to non-inductive current.

equation is solved analytically, (3) geometric factor of Ohkawa current is calculated, and (4) neoclassical conductivity is calculated. And the FIT code [10] has the following characteristics; (1) birth profile calculation of high energy particle including 3D geometry, (2) high energy particle energy deposition profile averaged over magnetic surface including the deviation of particle orbit from birth radial position, and (3) slowing down process is taken into account by using the steady state solution of Fokker-Plank equation.

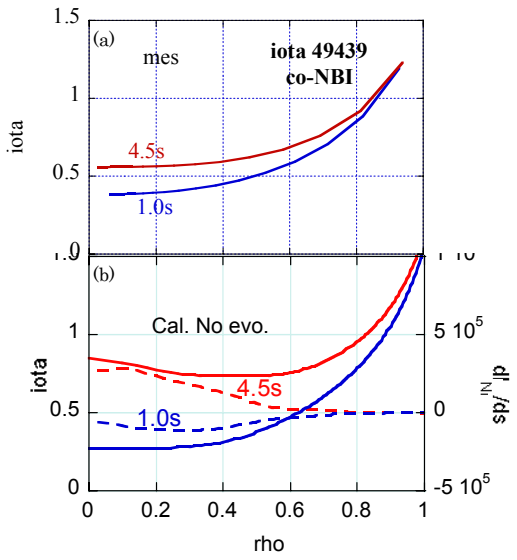

Fig.3 Rotational transform profile at the beginning of the discharge, t = 1.0s, and near to the end, t = 4.5s: (a) measured rotational transform profile, (b) non-inductive current profile (dashed) and the rotational transform profile due to non-inductive current estimated by the calculation.

As is shown in Ref. [1], Fig.2 shows a waveform of the discharge with 2 neutral beam (NB) injection. The 1st NB is injected to the counter-direction from $t \sim 0.7$ s and the 2nd NB to the co direction from $t \sim 1.2$ s. Here non-inductive current driven by the NB injection to the co-direction increases vacuum rotational transform. In Fig. 2(a), the blue line denotes the observed net toroidal current by Rogowski coils. Dotted line and dashed line denote the absorbed NB power for co-injection and counter-injection, respectively (its absolute value corresponds to the power). The calculated non-inductive current is shown by the red line for both Ohkawa and bootstrap current and by the green line for Ohkawa current. The difference between the blue and red lines corresponds to the inductive current due to the self-inductance induced voltage. Figure 2(b) and (c) show the averaged beta value, the electron density and the rotational transform measured by MSE [11]. Since plasma beta is low in this discharge, BS current is negligibly small and Ohkawa current is dominant for the non-inductive current. Figure 2(d) shows the evolution of the estimated rotational transform due to non-inductive current. The measured rotational profile at the beginning of the discharge, $t \sim 1.0$ s, and near to the end, $t \sim 4.5$ s are shown in Fig. 3(a). Figure 3(b) shows the profile of non-inductive current, dI_{NI}/ds (dashed lines) and the rotational profile due to the non-inductive current (solid lines) estimated by the calculation, where s is a normalized toroidal flux. It is shown by the results in Fig.2 and 3 that the inductive current is important to suppress the rapid change of plasma current due to the non-inductive current introduced abruptly by the NB injection. However, the fact that the difference between the observed current and the calculated non-inductive current is gradually decreased with time indicates that the numerical calculation of Ohkawa current and the bootstrap current by the combination of VMEC and BSC/FIT modules can explain the non-inductively driven current in LHD (contribution of the bootstrap current is negligible for this particular example of a low beta plasma).

4. Inductive currents in helical plasmas

The time evolution of the inductive plasma current corresponds to the resistive evolution of magnetic flux, and is posed in terms of the rotational transform ι. For the general non-axisymmetric toroidal configurations, Strand and Houlberg [12] describe the rotational transform evolution as

$$\left.\frac{\partial \iota}{\partial t}\right|_{\rho=const} = \left[\frac{\partial \Phi_T}{\partial \rho}\right]^{-1}\left[\frac{\partial \iota}{\partial \rho}\frac{\partial \Phi_T}{\partial t}\right|_{\rho=const} + \frac{\partial}{\partial \rho}\left\{\eta_{\parallel}\frac{\partial \Phi_T}{\partial \rho}\left(S_{21}\iota + S_{22}\right)^2\frac{\partial}{\partial \rho}\left[\frac{S_{11}\iota + S_{12}}{S_{21}\iota + S_{22}}\right] - \eta_{\parallel}\left[\frac{\partial \Phi_T}{\partial \rho}\right]^{-1}\frac{\partial V}{\partial \rho}\left\langle \boldsymbol{J_s}\cdot\boldsymbol{B}\right\rangle\right\}\right]$$

where ρ, Φ_T, V, $\eta_{\parallel}$, and $\left\langle \boldsymbol{J_s}\cdot\boldsymbol{B}\right\rangle$ denote radial coordinate, toroidal flux, volume inside the flux surface, resistivity, and flux surface averaged non-inductive parallel current, respectively. When the magnetic field is written as $\boldsymbol{B} = \Phi_T{}'\nabla\rho\times\nabla\left(\theta + \lambda(\rho,\theta,\zeta) - \iota\zeta\right)$ in a flux coordinates (ρ,θ,ζ), the geometrical parameters or susceptance matrix elements

$$S_{11} = \frac{V'}{4\pi^2}\left\langle\frac{g_{\theta\theta}}{g}\right\rangle,$$

$$S_{12} = \frac{V'}{4\pi^2}\left\langle\frac{g_{\theta\zeta}(1+\partial_\theta\lambda) - g_{\theta\theta}\partial_\zeta\lambda}{g}\right\rangle,$$

$$S_{21} = \frac{V'}{4\pi^2}\left\langle\frac{g_{\zeta\theta}}{g}\right\rangle,$$

$$S_{22} = \frac{V'}{4\pi^2}\left\langle\frac{g_{\zeta\zeta}(1+\partial_\theta\lambda) - g_{\zeta\theta}\partial_\zeta\lambda}{g}\right\rangle,$$

are calculated from a magnetic stream function λ, the Jacobian of the transformation from flux coordinates to Cartesian coordinates $\sqrt{g}$, and the metric tensor elements $g_{\theta\theta}$, $g_{\theta\zeta} = g_{\zeta\theta}$, $g_{\zeta\zeta}$ obtained in the MHD equilibrium calculation. The prime denotes derivative with respect to ρ. The magnetic stream function λ is a periodic function of θ and ζ, and is retained for keeping choice of flux coordinates. In a straight magnetic field line coordinate system such as Boozer coordinates, λ is zero. Boozer coordinate system is one candidate to be adopted in this study because we have already use Boozer coordinates in the BSC/FIT code. A disadvantage to use Boozer coordinates is that Fourier spectra of quantities such as magnetic field strength on a flux surface become wider in Boozer coordinates than those in a coordinate system used in VMEC code (VMEC coordinates), especially when Shafranov shift is large. Moreover, the equation of the rotational transform is a one dimensional equation and all quantities in the equation are flux surface averaged or surface quantities, and Boozer coordinate system has few advantages in this calculation. Therefore we use VMEC coordinates in this study. In an axisymmetric configuration, $g_{\theta\zeta} = g_{\zeta\theta}$ and $\partial_\zeta\lambda$ becomes zero, and therefore $S_{12} = S_{21} = 0$. This means that the rotational transform equation becomes a diffusion-type equation of ι for axisymmetric plasmas. The relation between net toroidal current I_T and the rotational transform is given by

$$\iota = \frac{I_T}{S_{11}\Phi_T{}'} - \frac{S_{12}}{S_{11}}.$$

Since S_{12} and S_{21} are zero in an axisymmetric configuration, the rotational transform is proportional to the net toroidal current (the rotational transform is created only by the plasma current) and a diffusion equation of the net toroidal current can be obtained for a tokamak plasma, which is familiar in a tokamak transport code.

Though the rotational transform equation is not a linear equation of ι because the geometrical parameters are functions of ι through the equilibrium even in the axisymmetric case, the diffusion-type equation of ι for tokamak plasmas is easy to be solved numerically together

with the other transport equations, which are also diffusion-type equations (geometrical parameters determined by the MHD equilibrium would be assumed to be slowly evolving variables in many cases). However, the rotational transform equation for a non-axisymmetric configuration is explicitly nonlinear equation of ι. So, it is considered that another form of the rotational transform evolution is preferable for the numerical point of view. We found that if we use the MHD equilibrium condition,

$$-p'V' = \left(I_P' + \iota I_T'\right)\Phi_T'$$

and

$$\left\langle B^2 \right\rangle V' = \left(I_P + \iota I_T\right)\Phi_T',$$

diffusion-type equation of ι can be obtained even in the non-axisymmetric case as

$$\frac{\partial \iota}{\partial t} = \frac{1}{4\rho\Phi_{Ta}{}^2}\left[\frac{\partial}{\partial\rho}\left\{\eta_{\parallel}\frac{dV}{d\rho}\frac{\left\langle B^2\right\rangle}{\rho^2}\frac{\partial}{\partial\rho}\left[\rho\left(S_{11}\iota + S_{12}\right)\right]\right\} + \frac{\partial}{\partial\rho}\left\{\eta_{\parallel}\frac{dV}{d\rho}\frac{1}{\rho}\frac{dp}{d\rho}\left(S_{11}\iota + S_{12}\right) - \eta_{\parallel}\frac{dV}{d\rho}\frac{1}{\rho}\left\langle \boldsymbol{J}_s\cdot\boldsymbol{B}\right\rangle\right\}\right],$$

where we use the square root of the normalized toroidal flux as radial coordinate ρ and assume total toroidal flux at the plasma boundary Φ_{Ta} to be constant in time. In this equation, $\left\langle B^2\right\rangle$ and p' are entered instead of S_{21} and S_{22}. When we assume all the equilibrium quantities are slowly evolving quantities, we can use implicit difference scheme like Crank-Nicholson scheme to solve this equation numerically. We use the boundary condition of $\partial\iota/\partial\rho = 0$ (at $\rho = 0$) and assume $I_T(t)$ is given at the plasma boundary.

In order to check the numerical code for the rotational transform, Ohmic current ramp-up simulation is done for an LHD plasma. Figure 4(a) shows the specified time evolution of the total plasma current as input. In this simulation, we use a fixed 3D MHD equilibrium and set the non-inductive current to zero. Obtained net pararell current profile is shown in Fig.4(b). It takes about 5s for current penetration.

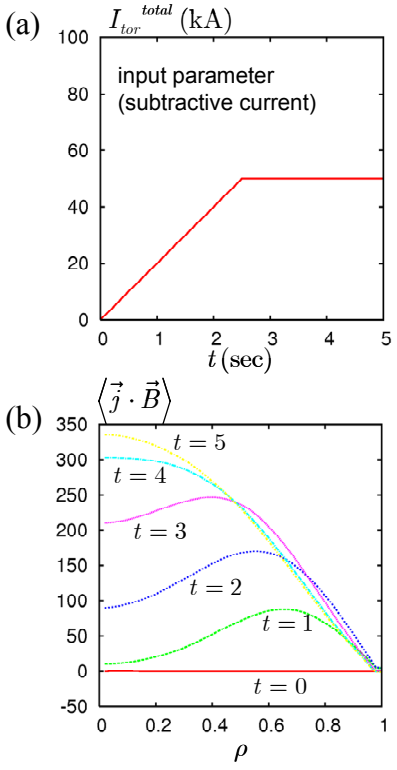

Fig.4 Current ramp-up simulation for an LHD plasma.

Numerical simulations are done for an LHD neutral beam heated plasma shown in Figs. 2 and 3. In this simulation, non-inductive current $\left\langle \boldsymbol{J}_s\cdot\boldsymbol{B}\right\rangle$ (Ohkawa current and bootstrap current in this case) is calculated by BSC/FIT code. First, calculation is done using a fixed MHD equilibrium and a fixed non-inductive current profile. As a boundary condition, time evolution of the total current is given by the experimental data (the blue line in Fig.2(a)). Results are shown in Fig.5 and 6. It is shown that the abrupt increase of plasma current by Ohkawa current is suppressed by the inductive component of the plasma current. Because of the finite resistivity, the total net current gets close to the non-inductive current with time.

Finally, time evolution of the rotational transform profile is solved self-consistently. In this simulation,

we use the time evolution of the total plasma current, the plasma density profile, and temperature profiles observed in the experiments. The fixed-boundary MHD equilibrium and the non-inductive current are updated at the sufficiently short time interval. Obtained time evolution of the rotational transform profile is shown in Fig. 7. In this simulation, the neoclassical conductivity calculated in the BSC code is used in the diffusion equation of the rotational transform. The increase of the central rotational transform is larger than that observed by MSE measurement. Free-boundary MHD equilibrium calculations are necessary to understand the reason clearly.

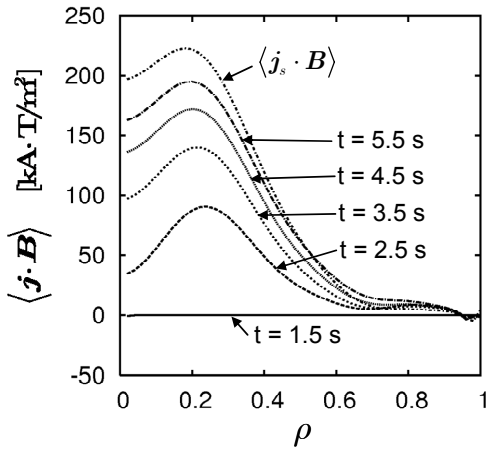

Fig.5 Time evolution of net plasma current profile in an LHD NB heated plasma.

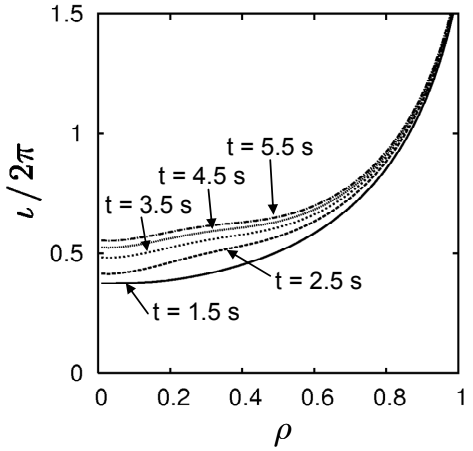

Fig.6 Time evolution of rotational transform profile in an LHD NB heated plasma.

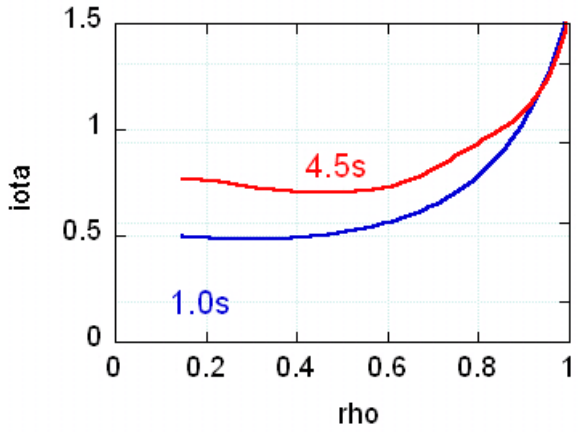

Fig.7 Time evolution of net plasma current profile in an LHD NB heated plasma.

5. Summary

Effects of the non-axisymmetry on the bootstrap (BS) current are investigated for a tokamak plasma having toroidal field (TF) ripples by using asymptotic expression of the neoclassical transport theory. It is found that the BS current is reduced by a factor of a square root of the TF ripple ratio in a rippled tokamak. These results suggest that the effect of the TF ripple on the bootstrap current is particularly important when the pressure gradient is steep near the plasma edge. If we lower the toroidicity (inverse aspect ratio), reduction of the bootstrap current due to

TF ripples is more pronounced. The effect of the safety factor on bootstrap current reduction due to TF ripples is weak. We also found that the reduction of the BS current due to TF ripple becomes small if we take the poloidal dependence of the TF ripple ratio into account.

For helical plasmas, we have developed a net plasma current simulation code for integrated simulations, and analyze net plasma currents observed in a Large Helical Device (LHD) plasma. It is found that non-inductive currents can be sufficiently large to change the rotational transform profile at the plasma core region, even though the total current is too small to change the rotational transform at the plasma boundary. The effect of the inductive current is important for estimation of the net plasma current especially when the beam driven currents are considered. Formulation of the time evolution of the rotational transform profile which is suitable for the numerical simulation is obtained to calculate inductive toroidal current in the presence of non-inductive current. A self-consistent simulation of the rotational transform profile has been done. The results obtained by using fixed-boundary MHD equilibria shows that the increase of the central rotational transform is larger than that observed by MSE measurement. Free boundary MHD equilibrium calculations are necessary to understand the reason clearly.

Acknowledgments

This work is supported by the 21st Century COE program “Establishment of COE on Sustainable Energy System” from the MEXT, Japan, and the LHD Coordinated Research program of NIFS (NIFS05KOAH020).

References

[1] Yuji Nakamura, et al., Fusion Science and Technology, **50** (2006) 457.
[2] K. C. Shaing and J. D. Callen, Phys. Fluids, **26** (1983) 3315.
[3] K. C. Shaing, et al., Phys. Fluids, **B1** (1989) 1663.
[4] K. Y. Watanabe, et al., Nuclear Fusion **32** (1992) 1499.
[5] K. Y. Watanabe, et al., Nuclear Fusion **35** (1995) 335.
[6] Yuji Nakamura, et al., Fusion Science and Technology, **50** (2006) 281.
[7] Yuji Nakamura, Plasma and Fusion Research, **1** (2006) 010.
[8] K. C. Shaing, et al., Phys. Fluids, **29** (1986) 2548.
[9] K. C. Shaing, et al., Phys. Fluids, **29** (1986) 521.
[10] S. Murakami, et al., Trans. Fusion Technol., **27** (1995) 259.
[11] K. Ida, et al., Rev. Sci. Instrum. **76**, 053505 (2005).
[12] P. I. Strand and W. A. Houlberg, Phys. Plasma, **8** (2001) 2782.